iScience, Volume *25*

Supplemental information

The vesicular transporter STX11 governs ATGL-mediated hepatic lipolysis and lipophagy

Gaojian Zhang, Jianxiong Han, Lili Wang, Xuegang Yang, Zhongkang Yan, Min Qu, Huijuan Zhou, Hazrat Bilal, Feifei Wang, Honghua Ge, and Xingyuan Yang

Supplemental Information

Supplemental figures

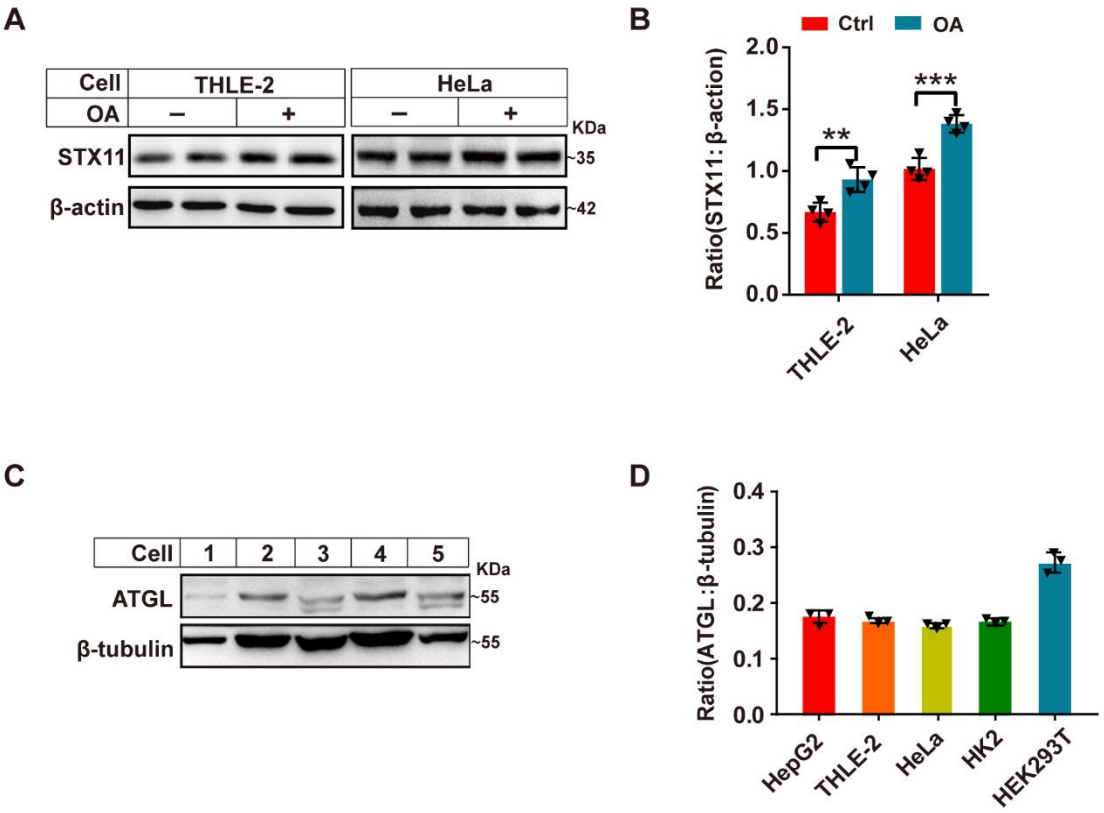

Figure S1. STX11 mediates lipid metabolism in vitro. Related to Figure 1.

(A) Endogenous STX11 protein in lysates from THLE-2 and HeLa cells treated with OA (400 μM) for 24 h was measured by immunoblotting. β-actin was used as the loading control.

(B) Relative expression of endogenous STX11 protein after different treatments.

(C) Cellular distribution of ATGL protein assessed by immunoblotting analysis. 1, HepG2; 2, THLE-2; 3, HeLa; 4, HK2; 5, HEK293T. β-tubulin was used as the loading control.

(D) Relative expression of ATGL in different cells.

Data are shown as mean ± SEM (n=3). **p < 0.01, *p < 0.001, t test.

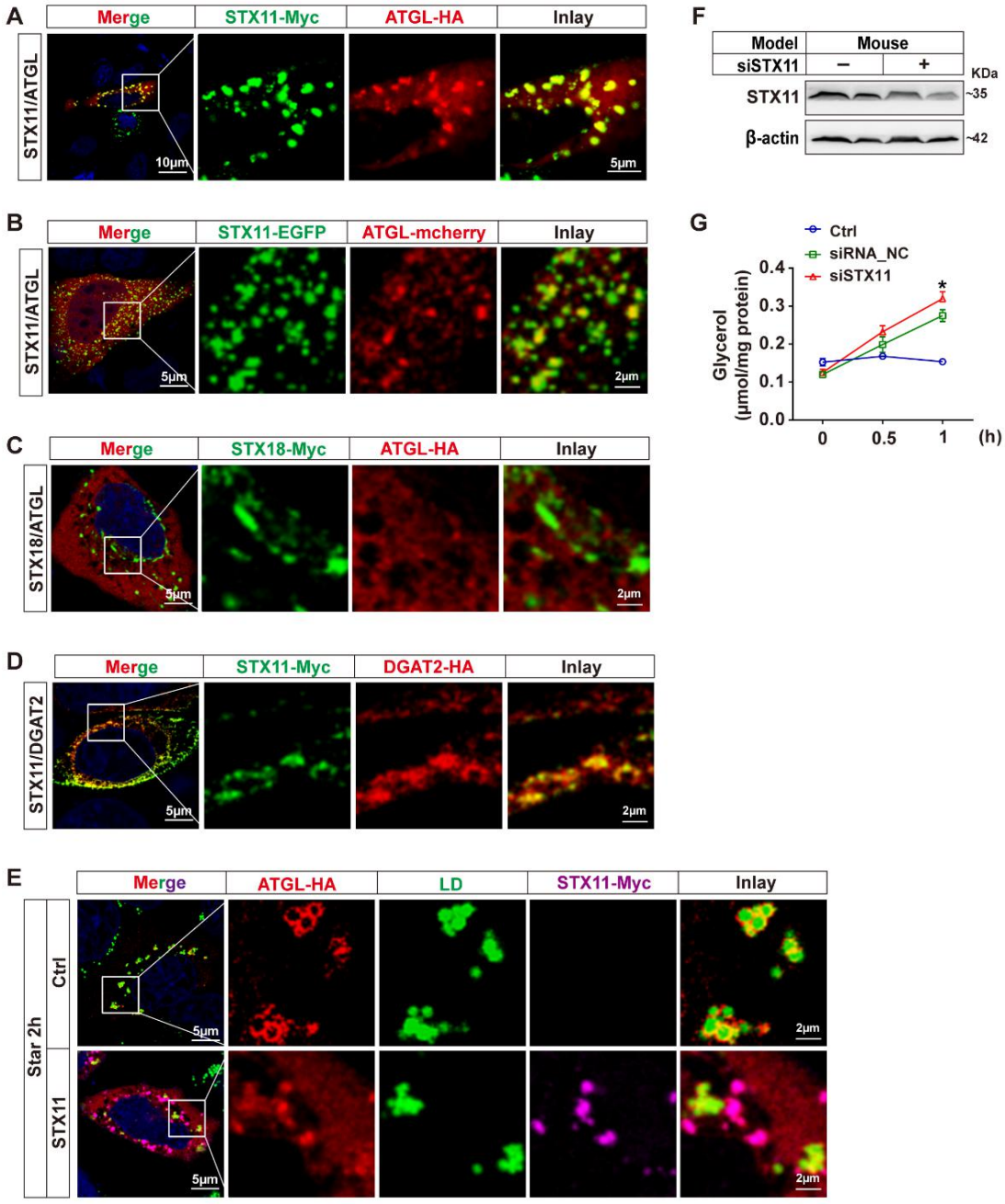

Figure S2. STX11 affects the spatial localization of ATGL in THLE-2 cells. Related to Figure 2 and Figure 4 and Figure 5.

(A and B) Co-localization of STX11 and ATGL in THLE-2 cells. Cells were co-transfected with ATGL-HA and STX11-Myc (A) or STX11-EGFP and ATGL-mcherry (B) were incubated under normal growth conditions. Immunofluorescence staining with anti-HA and anti-Myc antibodies was performed to reveal colocalization between ATGL-HA (red) and STX11-Myc (green) (A).

(C) No co-localization of STX18 and ATGL. THLE-2 cells were co-transfected with ATGL-HA and STX18-Myc. ATGL-HA proteins immunofluorescence staining were performed by using anti-HA (red) and STX18-Myc proteins were stained with anti-Myc (green) antibodies.

(D) Co-localization of STX11 and DGAT2 in THLE-2 cells. STX11-Myc and DGAT2-HA proteins were subjected

to immunostaining with anti-Myc (green) and anti-HA (red) antibodies.

(E) Representative images and quantification of ATGL co-localization with LDs demonstrate that STX11 prevents ATGL movement to the surface of LDs in THLE-2 cells. STX11-Myc proteins immunofluorescence staining was performed by using anti-Myc (violet) and ATGL-HA proteins were stained with anti-HA (red) antibodies. Lipid droplets were stained with BODIPY 493/503 fluorescent dye. All experiments were performed three times.

(F and G) In vivo siRNA-mediated knockdown of STX11 in mice liver was achieved by tail-vein injection every 3 days for 4 weeks with either control siRNA or STX11-targeting siRNA (1 mg/kg) (General Biol, China). One month later, 0.1g hepatic tissues extract was incubated with substrate TG (Sigma-Aldrich #LRAC2657) for 30 min, 60 min, and glycerol release was measured and normalized with the total protein levels in the extracts. Expression of STX11 protein was analyzed by immunoblotting, using β-actin as a loading control. Data are shown as mean ± SEM (n=3). *$p < 0.05$, t test.

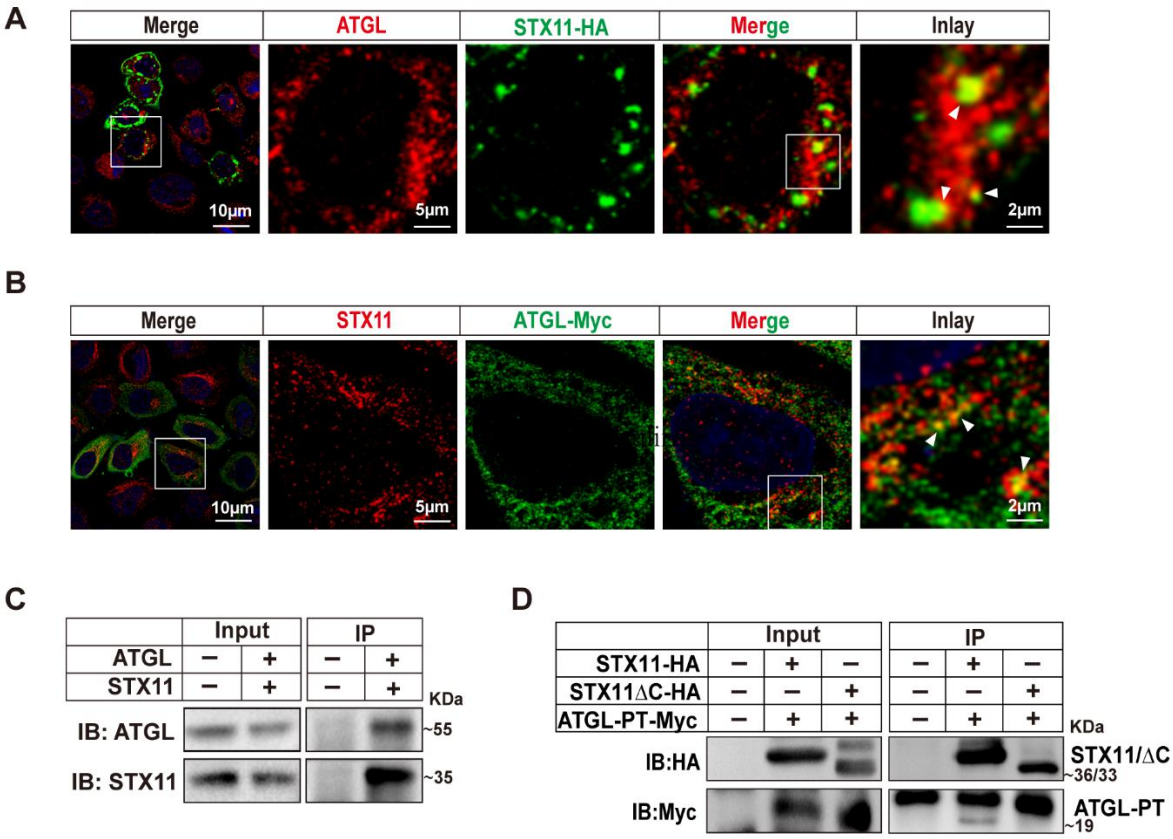

Figure S3. STX11 interacts with ATGL. Related to Figure 2 and Figure 3.

(A) Representative image analysis of endogenous ATGL co-localization with STX11-HA in HeLa cells. ATGL was stained with anti-ATGL (red) and STX11 was stained with anti-HA (green) antibodies. Yellow sections indicate colocalization (white arrows).

(B) Representative image analysis of endogenous STX11 co-localization with ATGL-Myc in HeLa cells. ATGL was stained with anti-Myc (green) and STX11 was stained with anti-STX11 (red) antibodies. Yellow sections indicate colocalization (white arrows).

(C) Endogenous immunoprecipitation with STX11 and ATGL in THLE-2 cells. STX11 proteins were immunoprecipitated using STX11 antibodies. STX11 and ATGL proteins in both the immunoprecipitates and lysates were detected by immunoblotting using STX11 and ATGL antibodies.

(D) C-terminal of STX11 interacts with PT domain of ATGL. HEK293T cells were co-transfected with ATGL-PT-Myc together with different STX11 constructs (ATGL-PT-Myc+STX11-HA, ATGL-PT-Myc+STX11ΔC). STX11 proteins were immunoprecipitated with anti-HA antibodies. STX11 and ATGL proteins in immunoprecipitates and lysates were detected by immunoblotting with HA and Myc antibodies.

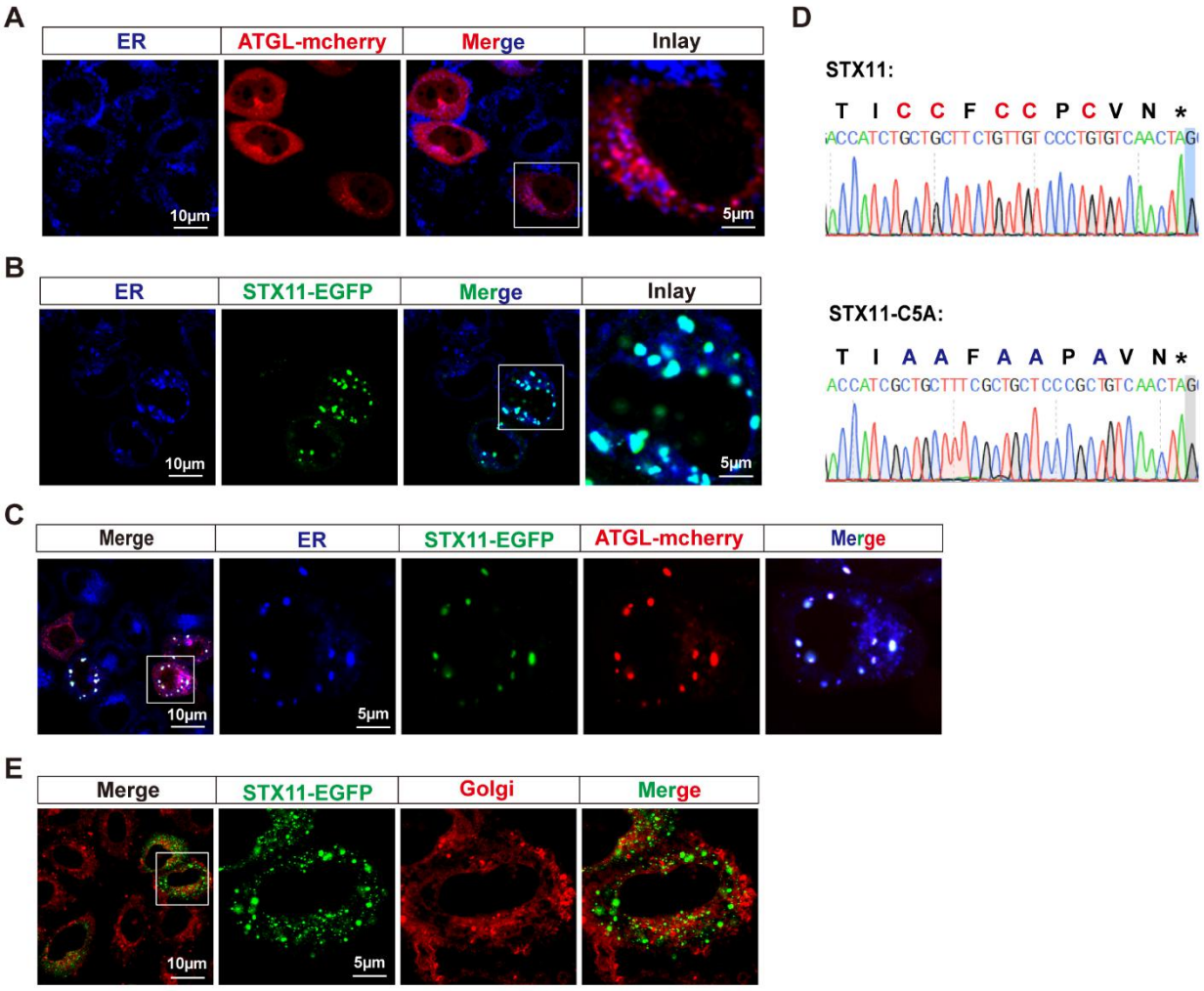

Figure S4. Colocalization of STX11 with ATGL on ER in HeLa cells. Related to Figure 6.

(A) No co-localization of ATGL with the ER. HeLa cells were transfected with ATGL-mcherry and the ER was stained with ER-Tracker Blue-White DPX followed by confocal microscopic analysis.

(B) STX11 localizes to the ER. HeLa cells were transfected with STX11-EGFP and then the ER was stained with the ER-Tracker Blue-White DPX.

(C) Analysis of confocal microscopy demonstrate co-localization of STX11 with ATGL at the ER. STX11-EGFP and ATGL-mcherry were co-transfected into HeLa cells and the ER was stained with ER-Tracker Blue-White DPX.

(D) DNA sequencing chromatogram of plasmids showing a mutation in the C-terminal region of STX11. 5 Cys were mutated to Ala.

(E) No co-localization of STX11 with the Golgi. Hela cells were transfected with STX11-EGFP and Golgi was stained with Golgi-Tracker Red. Immunofluorescence was analyzed by confocal microscopy.

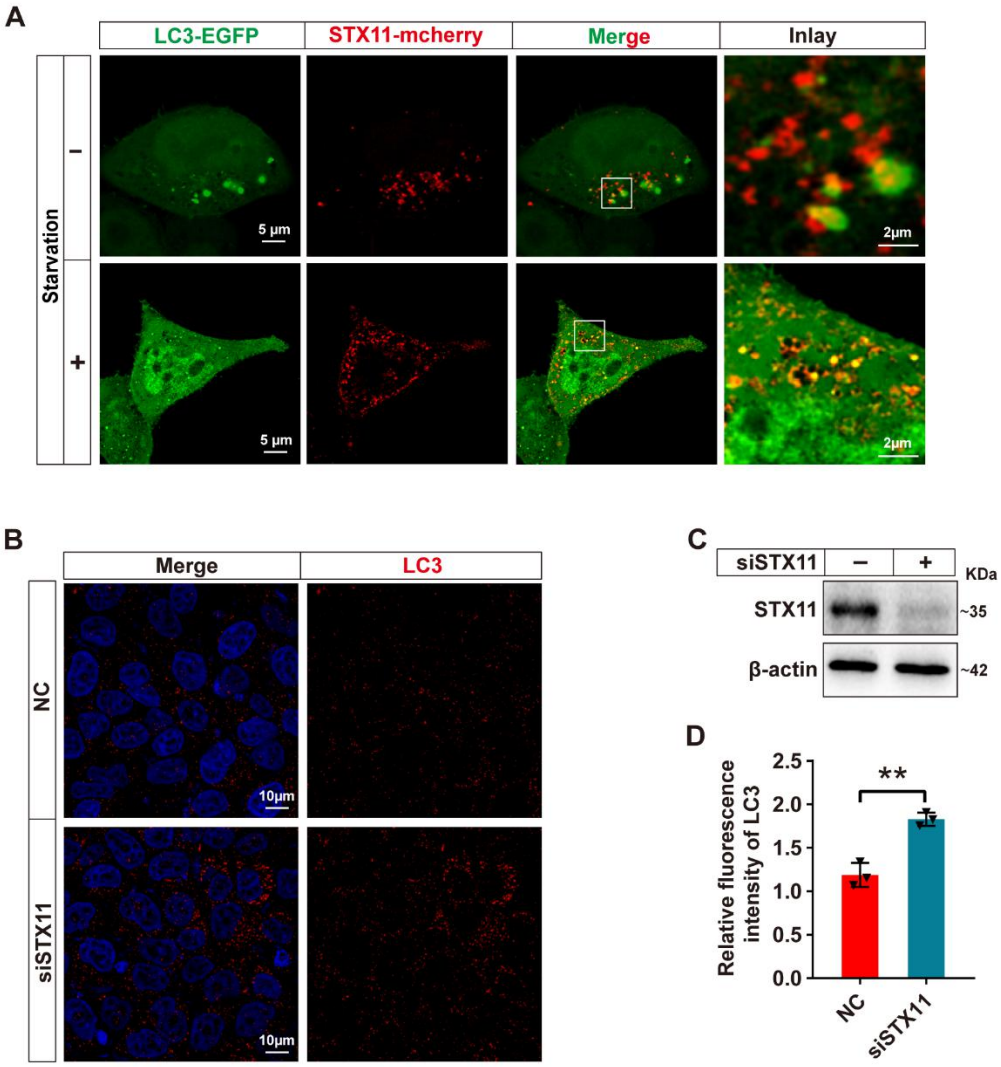

Figure S5. STX11 is involved in autophagy/lipophagy in HeLa cells. Related to Figure 7.

(A) STX11 co-localizes with LC3 under starvation conditions. HeLa cells were co-transfected with STX11-mcherry and LC3-EGFP. Cells were subjected to starvation (4 h) or no starvation followed by confocal microscopic analysis.

(B and C) Representative confocal microscopy images showing the LC3 in siSTX11 HeLa cells and control HeLa cells. Cells were starved for 4 h. LC3 protein immunofluorescence staining was performed using anti-LC3B (red). Protein expression was analyzed by immunoblotting using anti-STX11 antibodies. β-actin was used as the loading control.

(D) Quantification of LC3 fluorescence intensity from confocal microscopic images. Data are shown as mean ± SEM (n=3). **p < 0.01, t test.

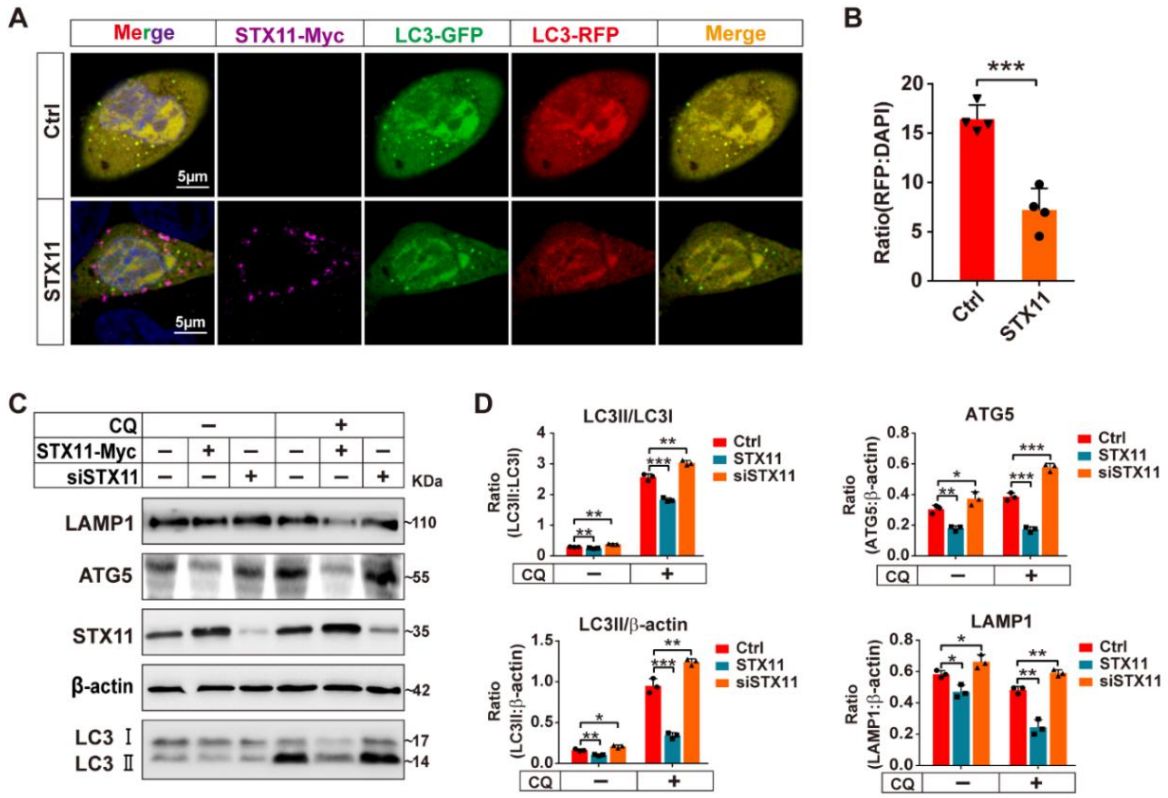

Figure S6. STX11 affects the autophagy pathway in hepatocytes. Related to Figure 7.

(A) THLE-2 cells were co-transfected with the dual RFP-GFP-LC3 plasmid and STX11-Myc plasmid. Confocal microscopy analysis showed decreased red punctate are indicative of reduced lysosomal activity as observed with the STX11 overexpress cells when compared to control cells (n=4) **(B)**.

(C) STX11 is involved in the autophagy pathway. Immunoblotting of THLE-2 cells transfected with STX11-Myc or Knockdown of STX11. Cells were treated with chloroquine (CQ 100 μM, Sigma-Aldrich #105M4035V) 12 h. Protein form cell lysates were detected by immunoblotting with anti-STX11, anti-LAMP1, anti-ATG5, and anti-LC3B antibodies.

(D) Quantification of the protein level under the normal and CQ conditions. β-actin was used as the loading control for the immunoblots and the data are shown as mean ± SEM (n=3). *p < 0.05, **p < 0.01, ***p < 0.001, t test.

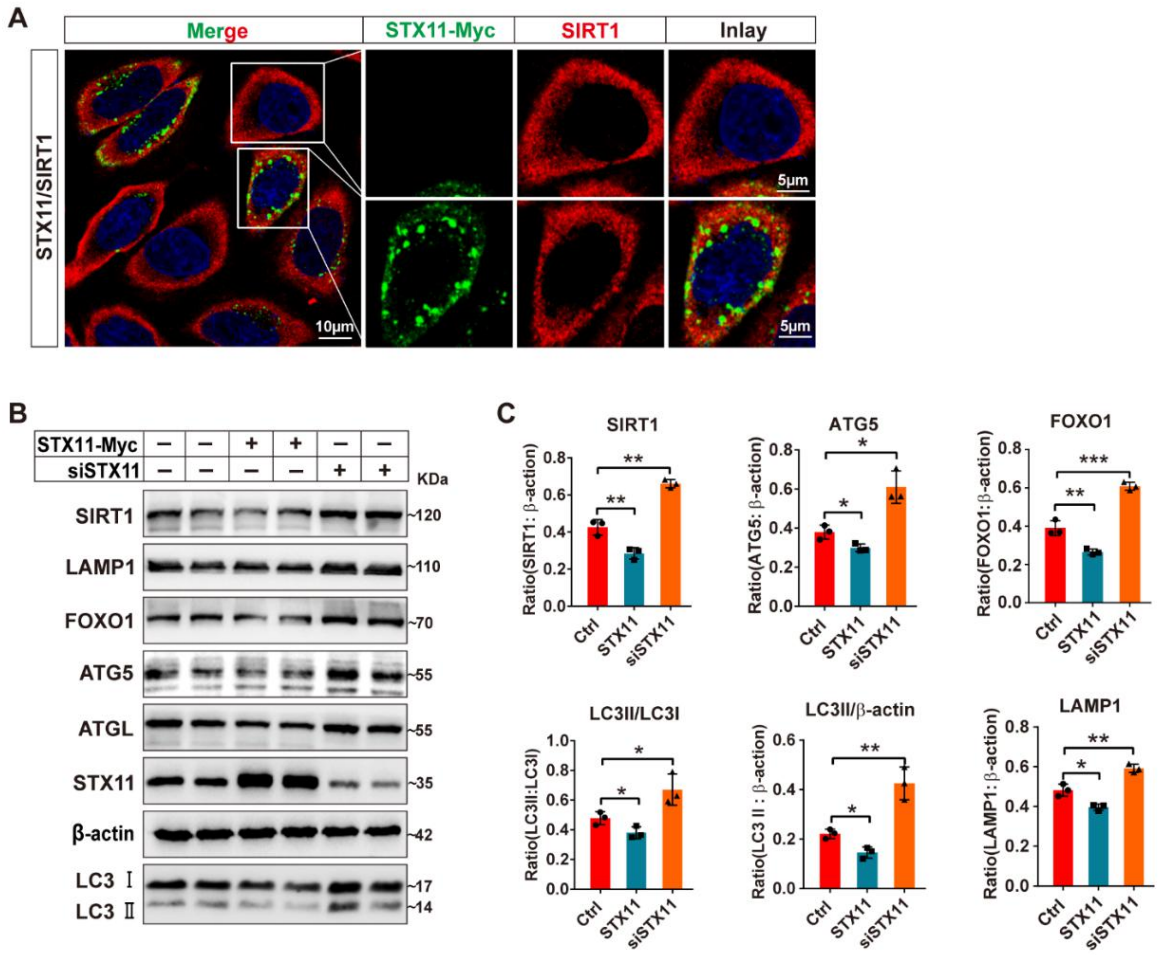

Figure S7. STX11 is involved in the SIRT1 mediated lipophagy pathway. Related to Figure 7.

(A) No co-localization of STX11 and SIRT1. THLE-2 cells were transfected with STX11-Myc. SIRT1 proteins immunofluorescence staining were performed by using anti-SIRT1 (red) and STX11-Myc proteins were stained with anti-Myc (green) antibodies.

(B) Immunoblotting of THLE-2 cells transfected with STX11-Myc or Knockdown of STX11. Cells were treated with OA (400 μM) 24 h following serum-free starvation for 2 h. Protein from cell lysates were detected by immunoblotting with anti-SIRT1, anti-FOXO1, anti-ATG5, anti-STX11, anti-LAMP1, anti-ATGL, and anti-LC3B antibodies.

(C) Relative expression of different lipophagy-related proteins in B. β-actin was used as the loading control for the immunoblots. Data are shown as mean ± SEM (n=3). *p < 0.05, **p < 0.01, ***p < 0.001, t test.

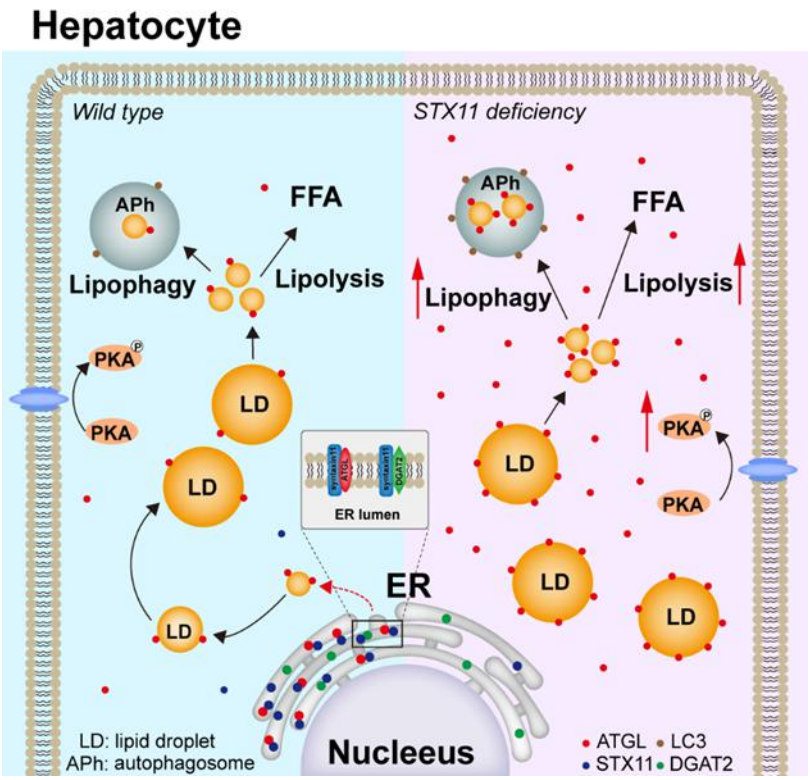

Figure S8. Role of STX11 in lipolysis and lipophagy. Related to Figure 7.

Under normal conditions, ATGL is bound to the ER through STX11, maintaining hepatocyte homeostasis, and lipolysis and lipophagy were processed normally. Upon knockdown of STX11 in hepatocytes, ATGL translocates from the ER to LDs, and promotes lipolysis and lipophagy.